MECHANIKA TEORETYCZNA
I STOSOWANA
Journal of Theoretical
and Applied Mechanics
1, 35, 1997

AIRCRAFT STABILITY ANALYSIS FOR STRONGLY COUPLED AERODYNAMIC CONFIGURATION

ZDOBYSŁAW GORAJ

Institute of Aeronautics and Applied Mechanics, Warsaw University of Technology
e-mail: goraj@meil.pw.edu.pl

PIOTR KULICKI

MACIEJ LASEK

Institute of Aviation, Warsaw

Application of panel methods to flight dynamics analysis has been shown. The most important facts from panel methods theory (governing equations, boundary conditions forms, discretization methods etc.), having fundamental weight and making possible computing of the pressure distribution over the lifting and non-lifting surfaces, have been presented and discussed. Some numerical procedures for computing selected dynamic and aerodynamic characteristics, decisive from to stability point of view, namely downwash behind the main wing, stability and maneuverability neutral points and stability derivatives, have been discussed in details. Some results obtained numerically have been compared to those obtained from wind tunnels and by simplified engineering procedures.

Key words: flight dynamics, panel methods, stability

1. Introduction

Over the last two decades it can be observed that new, unconventional (unorthodox), strongly coupled aerodynamic configurations, have been build. More and more frequent are; e.g., Canard configurations, lifting bodies smoothly passing into wings, configurations of manifold control surfaces or with leading edge extensions. In a conventional approach to the stability and maneuverability analysis it is usualy assumed that the main wing is placed in an undisturbed uniform flow, a wing platform is of trapezoidal shape (no that of

hybrid) and that the body can be clearly separated from wing and tail etc. For unconventional configurations these assumptions do not hold true, therefore the stability derivatives, mostly those obtained numericaly, can be adulterated, so the stability and maneuverability characteristics could occur worthless. Experimental wind-tunnel investigations (e.g., Heffley and Jewell (1972)) or flight tests are time consuming and expensive, so they can only supplement and verify the data obtained numerically. In view of that it seems advisable to develop a method of computing of the aerodynamic characteristics for unconventional configuration, including the stability derivatives, using lifting surface integral equation. To this end the panel methods have been used. They consist in dividing the surfaces into small trapezoidal or triangular elements (panels) and distributing over these elements different type singularities (doublets, vortices and sources). Different versions of panel methods have been developed (cf Goraj and Pietrucha (1993), (1995a,b,c); Kubryński (1995); Kulicki and Lasek (1995a,b)). They differ mainly in kind of singularities to be used, form of singularities distribution (discrete or continuous) to be applied, wing thickness to be either included or excluded, shape of the wake (flat or rolling-up), etc. Depending on the method used a simpler or more complex mathematical model can be obtained. In the paper the following assumptions have been made: the flow around the aircraft is subcritical and potential (excluding the wake). Aircraft is either in steady, rectilinear, horizontal flight or in revolution with steady angular velocity. In both cases the angles of attack are small.

Moreover, disturbances around a steady trajectory are small. The wings can be modeled as either thick surfaces using doublets and sources or as thin surfaces using vortices. The bodies can be modeled as thick surfaces over which only sources are distributed. In all cases the singularities distribution is of constant strength. On the wake only doublets are used. The wake influences the lifting surfaces up to limited distance only – usually up to several wing chords (cf Goraj and Pietrucha (1994a,b)).

2. Mathematical model

The flow around aircraft can be described by the Laplace equation (cf Hess and Smith (1966); Hess (1972); Katz and Plottkin (1991))

$$\nabla^2 \Phi = 0 \tag{2.1}$$

with the boundary conditions

$$\lim_{r\to\infty}(\nabla\Phi - \boldsymbol{v}) = \mathbf{0} \tag{2.2}$$

$$\nabla\Phi \cdot \boldsymbol{n} = 0 \tag{2.3}$$

Solution of the Laplace equation has the form

$$\Phi(P) = -\frac{1}{4\pi}\int_{S_B}\left[\sigma\left(\frac{1}{r}\right) - \mu\frac{\partial}{\partial n}\left(\frac{1}{r}\right)\right] dS + \frac{1}{4\pi}\int_{S_W}\left[\mu\frac{\partial}{\partial n}\left(\frac{1}{r}\right)\right] dS + \Phi_\infty(P) \tag{2.4}$$

Solution (2.4) depends on the singularities distribution over the aircraft body and wake behind the aircraft. The aircraft surface (body, wings and tail surfaces) and wake surface have been approximated by the flat panel set with a constant singularities distribution over each panel.

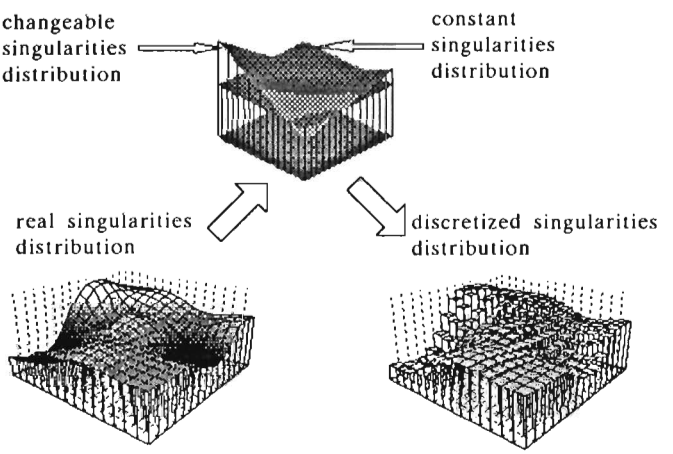

Fig. 1. Discretization of the real singularities distribution

After discretization, Eq (2.4) has the form

$$\Phi(P) - \Phi_\infty = \sum_{k=1}^{N_B}\frac{1}{4\pi}\int_{S_{\mu B}}\mu\boldsymbol{n}\cdot\nabla\left(\frac{1}{r}\right) dS + \tag{2.5}$$

$$+\sum_{l=1}^{N_W}\frac{1}{4\pi}\int_{S_{\mu W}}\mu\boldsymbol{n}\cdot\nabla\left(\frac{1}{r}\right) dS - \sum_{k=1}^{N_B}\frac{1}{4\pi}\int_{S_{\sigma B}}\sigma\left(\frac{1}{r}\right) dS$$

where

S_{μ_B}, S_{μ_W} – body and wake doublet panels, respectively
S_{σ_B} – body source panel.

Let us carry out ∇ operation (differentiation) over Eq (2.5). We obtain the vector equation in velocieties at the point P

$$\boldsymbol{V}(P) - \boldsymbol{V}_\infty = \sum_{k=1}^{N_B} \frac{1}{4\pi} \int_{S_{\mu_B}} \mu \nabla \Big[\frac{\partial}{\partial n} \Big(\frac{1}{r} \Big) \Big] \, dS + \tag{2.6}$$
$$+ \sum_{l=1}^{N_W} \frac{1}{4\pi} \int_{S_{\mu_W}} \mu \nabla \Big[\frac{\partial}{\partial n} \Big(\frac{1}{r} \Big) \Big] \, dS - \sum_{k=1}^{N_B} \frac{1}{4\pi} \int_{S_{\sigma_B}} \sigma \nabla \Big(\frac{1}{r} \Big) \, dS$$

Singularities strengths over panels are constant, so the integrals in Eq (2.6) can be written in the form of functions depending on panel geometry and singularity strength only. The part of the function depending on panel geometry is called the "panel influence coefficient". It can be defined either as potential (potential influence coefficient) or velocity (velocity influence coefficient), induced by a selected panel at a chosen P point on condition that the singularity strength is equal to unity. So, the potential influence coefficient is a scalar and the velocity influence coefficient is a vector. For example, the function under the first and second sums in Eq (2.5) can be written as

$$\frac{1}{4\pi} \int_{S_\mu} \mu \boldsymbol{n} \cdot \nabla \Big(\frac{1}{r} \Big) \, dS = f(\mu, geom) = \frac{1}{4\pi} \mu W_{\phi_\mu}(geom) \tag{2.7}$$

By virtue of Eq (2.7), Eqs (2.5) and (2.6) one can rewrite as

$$\begin{aligned} \Phi(P_i) - \Phi_\infty &= \frac{1}{4\pi} \sum_{k=1}^{N} \mu_k W_{\phi_{\mu k}}(P_i) + \frac{1}{4\pi} \sum_{l=1}^{N_W} \mu_l W_{\phi_{\mu l}}(P_i) + \\ &- \frac{1}{4\pi} \sum_{k=1}^{N} \sigma_k W_{\phi_{\sigma k}}(P_i) \end{aligned} \tag{2.8}$$

$$\begin{aligned} \boldsymbol{V}(P_i) - \boldsymbol{V}_\infty &= \frac{1}{4\pi} \sum_{k=1}^{N} \mu_k \boldsymbol{W}_{V_{\mu k}}(P_i) + \frac{1}{4\pi} \sum_{l=1}^{N_W} \mu_l \boldsymbol{W}_{V_{\mu l}}(P_i) + \\ &- \frac{1}{4\pi} \sum_{k=1}^{N} \sigma_k \boldsymbol{W}_{V_{\sigma k}}(P_i) \end{aligned} \tag{2.9}$$

Scalar equation (2.8) and three projections of vector equation (2.9) can be rewritten for N collocation points (in the area of different N panels on body

surface). After adding boundary conditions (also over N panels) we obtain the linear set of algebraic equations.

Boundary conditions can take different forms. For thick wings and bodies (3D) it is necessary to demand that the Dirichlet condition have to be fulfilled. Usually this condition takes the form $\Phi_i = \text{constant}$ (where Φ_i stands for the potential inside the body). Note that it is equivalent to the inner Neumann condition $\partial\Phi_i/\partial n = 0$ and it simply means that the potential inside the body will not change (cf Katz and Plottkin (1991)). If we put the value of potential inside the body Φ_i equal to the potential in outer flow in infinity, then Eq (2.8) takes the form

$$\sum_{k=1}^{N} \mu_k W_{\phi_{\mu k}}(P_i) + \sum_{l=1}^{N_W} \mu_l W_{\phi_{\mu l}}(P_i) = \sum_{k=1}^{N} \sigma_k W_{\phi_{\sigma k}}(P_i) \qquad i = 1, ..., N \quad (2.10)$$

For a infinitesimally thin surface it is sufficient to take the Neumann condition. Projection of Eq (2.9) on the directions normal to the surface yields

$$\sum_{k=1}^{N} \mu_k \boldsymbol{W}_{V_{\mu k}}(P_i)\boldsymbol{n}_i + \sum_{l=1}^{N_W} \mu_l \boldsymbol{W}_{V_{\mu l}}(P_i)\boldsymbol{n}_i = \sum_{k=1}^{N} \sigma_k \boldsymbol{W}_{V_{\sigma k}}(P_i)\boldsymbol{n}_i - 4\pi \boldsymbol{V}_\infty \boldsymbol{n}_i \quad (2.11)$$

In both cases Eq (2.10) or (2.11) one can rewrite in the following matrix form

$$\mathbf{W}_\mu \boldsymbol{\mu} = \mathbf{W}_\sigma \boldsymbol{\sigma} + \mathbf{C} \quad (2.12)$$

usefull for numerical solving.

The control (collocation) point (Fig.2) for doublet and source panels is usually placed in the center of flat panel. Moreover, when we put Dirichlet boundary condition, the control point is a bit shifted under panel surface in normal direction. A displacement is very small – in this paper the shifting is on six order magnitude less than the panel characteristic length.

For configurations composed of thick bodies and thin lifting surfaces one can apply respectively the so-called mixed boundary condition – on chosen part of the surface the Neumann condition stands up and on the other one the Dirichlet condition is imposed.

To determine the shape of wake one should solve the so-called inverse problem, in most cases by an iterative scheme. To avoid the iterative process one usually assumes an arbitrary, approximated wake geometry. In such a case no boundary condition is imposed over the wake. To obtain the singularities strengths over the wake one has to note that these strengths are related to those of distributed on body surface by means of Kutta-Joukowski condition,

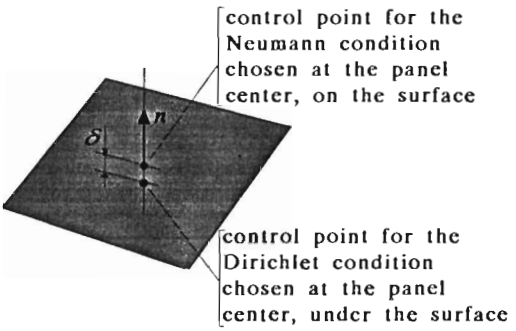

Fig. 2. Control point choosing

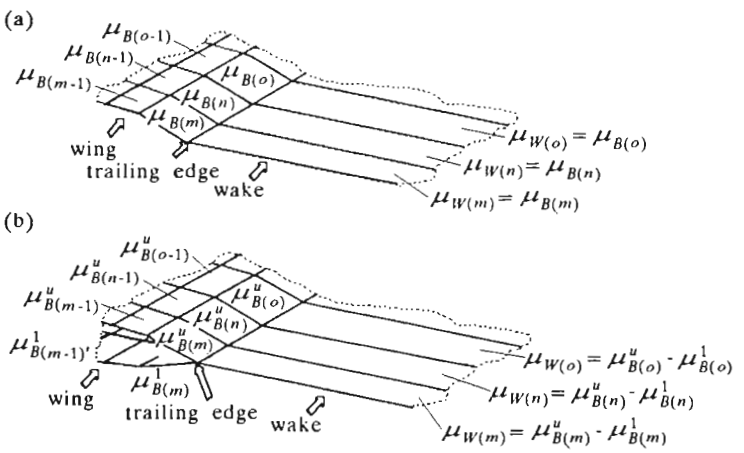

Fig. 3. One of possible versions of the Kutta-Joukowski condition for thin and thick wings

see Fig.3. It enables reduction of the number of unknown parameters and equations to the number of panels only on the aircraft surface.

Doublets and vortex rings are equivalent in the sense of induced velocities. So, the vortex rings can be used both on body and wakes instead of the doublets. For a steady flow the vortex rings used on the wake are equivalent to the horseshoe vortices (cf Katz and Plottkin (1991)).

3. Stability derivatives

Dimensional stability derivatives F_{ij} of the generalized aerodynamic force F_i (given in the velocity or stability frame of reference) with respect to the dimensional disturbance S_j (also given in the velocity or stability frame of reference) can be defined (cf Goraj (1984)) as

$$F_{ij} = \frac{\partial F_i}{\partial S_j} = \frac{\partial}{\partial S_j}\left(\frac{1}{2}\rho V^2 S l_i C_i\right) \tag{3.1}$$

where

l_i – characteristic length for the generalized force F_{ij} being an element of the set $\{1, 1, 1, b, c_a, b\}$

C_i – dimensionless force coefficient being an element of the set $\{-C_x, C_y, -C_z, C_l, C_m, C_n\}$.

From Eq (3.1) we obtain

$$\begin{aligned}
p_{11} &= x_u = -2C_x - \frac{\partial C_x}{\partial\left(\frac{u}{V}\right)} & p_{13} &= x_w = -\frac{\partial C_x}{\partial\left(\frac{w}{V}\right)} \\
p_{15} &= x_q = -\frac{\partial C_x}{\partial\left(\frac{qc_a}{V}\right)} & p_{31} &= z_u = -2C_z - \frac{\partial C_z}{\partial\left(\frac{u}{V}\right)} \\
p_{33} &= z_w = -\frac{\partial C_z}{\partial\left(\frac{w}{V}\right)} & p_{35} &= z_q = -\frac{\partial C_z}{\partial\left(\frac{qc_a}{V}\right)} \\
p_{37} &= z_{\dot{w}} = -\frac{\partial C_z}{\partial\left(\frac{\dot{w}c_a}{V^2}\right)} & p_{51} &= m_u = -\frac{\partial C_m}{\partial\left(\frac{u}{V}\right)} \\
p_{53} &= m_w = \frac{\partial C_m}{\partial\left(\frac{w}{V}\right)} & p_{55} &= m_q = -\frac{\partial C_m}{\partial\left(\frac{qc_a}{V}\right)} \\
p_{57} &= m_{\dot{w}} = -\frac{\partial C_m}{\partial\left(\frac{\dot{w}c_a}{V^2}\right)} & p_{22} &= y_v = \frac{\partial C_y}{\partial\left(\frac{v}{V}\right)} \\
p_{24} &= y_p = \frac{\partial C_y}{\partial\left(\frac{pb}{V}\right)} & p_{26} &= y_r = \frac{\partial C_y}{\partial\left(\frac{rb}{V}\right)} \\
p_{42} &= l_v = -\frac{\partial C_l}{\partial\left(\frac{v}{V}\right)} & p_{44} &= l_p = \frac{\partial C_l}{\partial\left(\frac{pb}{V}\right)} \\
p_{46} &= l_r = \frac{\partial C_l}{\partial\left(\frac{rb}{V}\right)} & p_{62} &= n_v = \frac{\partial C_n}{\partial\left(\frac{v}{V}\right)}
\end{aligned} \tag{3.2}$$

$$p_{64} = n_p = \frac{\partial C_n}{\partial\left(\frac{pb}{V}\right)} \qquad p_{66} = n_r = \frac{\partial C_n}{\partial\left(\frac{rb}{V}\right)}$$

Dimensional stability derivatives F_{ij} can be computed from dimensionless derivatives p_{ij} as follows

$$F_{ij} = \frac{1}{2}\rho S l_i l_j V^n p_{ij} \tag{3.3}$$

From Eq (3.3) we have

$$\begin{aligned}
X_u &= \frac{1}{2}\rho SV(-2C_x - C_{xu}) \\
X_w &= \frac{1}{2}\rho SVx_w & X_q &= \frac{1}{2}\rho Sc_aVx_q \\
Z_u &= \frac{1}{2}\rho SV(-2C_z - C_{zu}) & Z_w &= \frac{1}{2}\rho SVz_w \\
Z_q &= \frac{1}{2}\rho Sc_aVz_q & Z_{\dot{w}} &= \frac{1}{2}\rho Sc_az_{\dot{w}} \\
M_u &= \frac{1}{2}\rho Sc_aVm_u & M_w &= \frac{1}{2}\rho Sc_aVm_w \\
M_q &= \frac{1}{2}\rho Sc_a^2Vm_q & M_{\dot{w}} &= \frac{1}{2}\rho Sc_a^2m_{\dot{w}} \\
Y_v &= \frac{1}{2}\rho SVy_v & Y_p &= \frac{1}{2}\rho SbVy_p \\
Y_r &= \frac{1}{2}\rho SbVy_r & L_v &= \frac{1}{2}\rho SbVl_v \\
L_p &= \frac{1}{2}\rho Sb^2Vl_p & L_r &= \frac{1}{2}\rho Sb^2Vl_r \\
N_v &= \frac{1}{2}\rho SbVn_v & N_p &= \frac{1}{2}\rho Sb^2Vn_p \\
N_r &= \frac{1}{2}\rho Sb^2Vn_r
\end{aligned} \tag{3.4}$$

4. Surface paneling

Application of quadrilaterals in a panelization process very often leads to the twisted panels. A computational procedure is much simpler (cf Blaszczyk (1996)) if twisted panels are flatted-up, Fig.4.

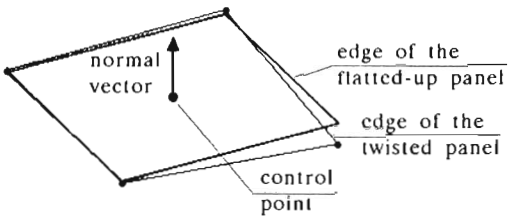

Fig. 4. Quadrilateral surface element (panel)

Aspect ratio can not be too high for each panel. Adjacent panels can not differ too much in shape. It is admissible that the panels deform into triangles. Some grids generate errors either at the stage of determination of the potential or at the stage of differentation of the potential, Fig.5.

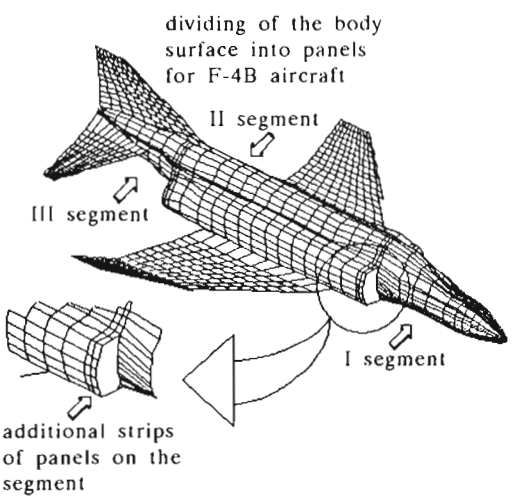

Fig. 5. Grid model showing surface dividing into segments

Particular body segments, between which a discontinuity occur, are treated as separated objects. Only the condition of node compatibility along the adjacent edges has to be fulfilled. It enables moving from one object to another when differentiating. Moreover, in the discontinuity region, some panel strips on the extreme edge are usually added. This way, dividing into panels in the direction perpendicular to the edge, is compressed. It results in a much smaller interpolation error appearing in the discontinuity region.

For a thin wing in the region connection with body the condition of consi-

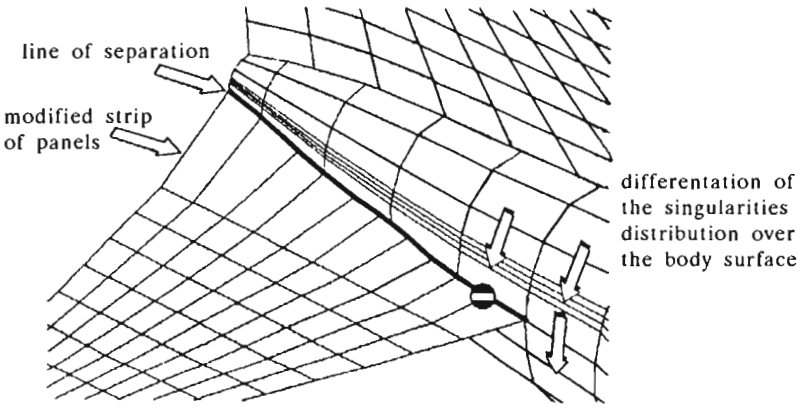

Fig. 6. Thick body – thin wing connection

stency between near the body chord and the body longeron has been imposed. It means that grids on the body longeron are consistent with the first and the last grids on near the body chord, Fig.6. It has made it possible to consider the body longeron section adjacent to the wing chord as a kind of body surface separation line (or as an "inner edge"). It means that numerical differentiation over the body surface is not performed "through the thin wing surface".

5. Stability derivatives for light executive aircraft

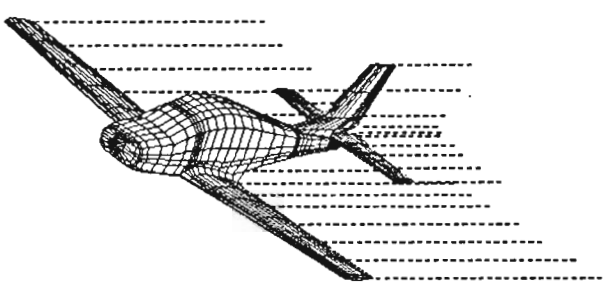

Fig. 7. Configuration of an executive aircraft

Stability derivatives have been calculated by means of three different methods: classical Hess method (cf Hess and Smith (1966)), Vortex Lattice Me-

thod (VLM) (cf Bertin and Smith (1989); Goraj (1993); Konstandinopoulos et al. (1985)) and simplified engineering method (cf Goraj (1984); [25]). Fig.7 presents a light aircraft and wakes behind it after paneling, performed on the basis of Hess method (about 1500 panels). Wake strips are also shown and denoted by dotted lines.

Some stability derivatives computed by means of the three abovemention methods are presented in Table 1.

Table 1

	m_q	z_q	m_w	z_w
simplified methods	−10.977	−7.153	−1.145	−5.942
VLM	−9.970	−5.590	−0.868	−5.400
Hess method	−10.850	−6.642	−1.146	−5.672

Lateral stability derivatives have been computed by means of the QL-Panel package (cf Kulicki and Lasek (1995c)). The results are shown in Table 2, the case, when the aircraft surface has been divided into 648 panels.

Table 2

	l_v	l_p	l_r	n_v	n_p	n_r
QL-Panel	−0.057	−0.288	0.0915	0.0611	−0.0366	−0.070
Wind-tunnel	−0.043			0.0773		

Analysing the stability derivatives presented in Table 1 and Table 2 it can be concluded that the methods under consideration lead to the results consistent with simplified engineering procedures (cf Goraj (1984); [25]) for longitudinal derivatives and with wind-tunnel measurement results for lateral derivatives, respectively.

6. Determination of neutral points of stability and maneuverability

Neutral points of an aircraft have to be computed as early as at the preliminary design stage with a relatively high accuracy (3% ÷ 5% of mean aerodynamic chord (MAC)). For simply, conventional configuration neutral points can be estimated using the ESDU [25] and only sometimes are verified by wind-tunnel investigations. For more complex configurations, in the case of; e.g., (1) strong, nonlinear wing twisting, (2) hybrid wing planform, (3) leading edge skip or extension, (4) strong negative leading edge sweep angle, or strongly coupled main and tail wings the ESDU can not be used and only

time-consuming and expensive wind-tunnel measurements can be applied. In view of that we decided to use panel methods for computing of stability and maneuverability neutral points.

The neutral points of stability and maneuverability for an aircraft can be defined as follows.

The neutral point with either fixed (NC) or with free (NF) elevator corresponds to the point around which the pitching moment is reduced that gradients of the piching moment with respect to either the angle of attack or the lifting force coefficient, respectively, are equal to zero in the linear range of angles of attack, i.e.

$$\frac{\partial C_m^{NC}}{\partial C_L} = 0 \qquad \frac{\partial C_m^{NF}}{\partial C_L} = 0 \tag{6.1}$$

Positions of the neutral points can be computed from the following formula

$$x_N = \frac{x_2 C_{L2} - x_1 C_{L1}}{C_{L2} - C_{L1}} \tag{6.2}$$

where

x – center of pressure position

C_L – lifting force coefficient, and indexes $1, 2$ correspond to two different angles of attack.

To compute the neutral point with a free elevator either the trimmer deflection or the stabilizer setting should be found earlier. Some details of NF (neutral point of stability with free elevator) or MC and MF (neutral points of maneuverability with fix or free elevator) can be found in Goraj et al. (1996). In Table 3 the neutral points of stability with fixed elevator obtained by means of the Hess method for different wings have been shown and compared with those obtained by simplified engineering methods from ESDU [25].

Table 3

λ, A	$\lambda = 0.5$, $A = 2.67$			$\lambda = 0.5$, $A = 5.33$			$\lambda = 1$, $A = 2$		
sweep	0°	30°	45°	0°	30°	45°	0°	30°	45°
Hess method	0.226	0.508	0.719	0.239	0.789	1.156	0.211	0.489	0.679
ESDU 70011	0.223	0.495	0.697	0.239	0.765	1.468	0.205	0.467	0.668

7. Downwash distribution

Downwash in the tail vicinity can be computed having singularities distri-

bution over the aircraft surfaces. Downwash at each point of the field can be found from the formula

$$\epsilon = -\arctan\left(\frac{1}{V_\infty}\frac{\partial \Phi}{\partial z}\right) \tag{7.1}$$

where $\partial\Phi/\partial z$ denotes the velocity induced by all singularities in the direction perpendicular to the undisturbed flow velocity.

Many different tests have been performed for various wake models (cf Katz and Plottkin (1991)) behind a thick wing of aspect ratio equal to 6, at the angle of attack equal to 5°. Downwashes (in deg) computed at the point ($x = 3c_a, y/2b = 0.3$) behind the wing and for various z coordinates (given in MAC percentage) are placed in Table 4 and in Fig.8. Wake is placed along the wing chord for the first model, and along the vector of undisturbed flow velocity for the second model, respectively. Differences between the results for various models are not significant (less than 0.5°) and can be accepted in stability analysis. It means that the extreme difference for the parameter $\partial\epsilon/\partial\alpha$, a very important one from the stability point of view, is less than 10%.

Table 4

Z coordinate	wake models		simplified calculations	
(in % of MAC)	model 1	model 2	ESDU [25]	Roskam [25]
−20	1.94	1.81	1.54	1.55
0	2.02	1.92	1.94	1.67
+20	1.95	2.02	2.08	1.55

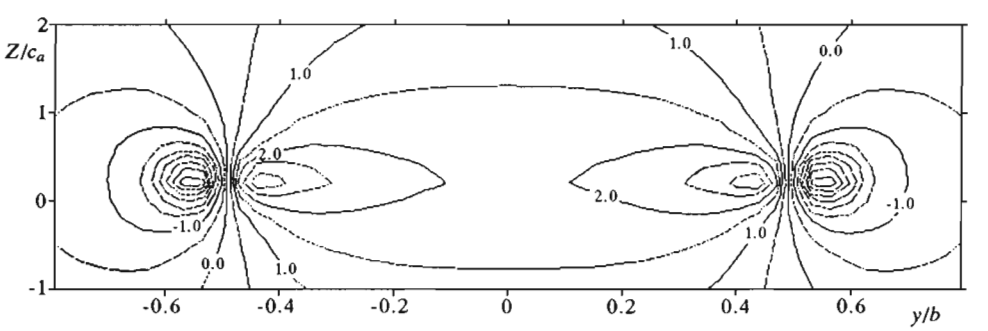

Fig. 8. Downwash izolines behind the rectangular wing of aspect ratio 6

Downwashes obtained for F-4B aircraft (Fig.9) with the aid of QL-Panel package (cf Kulicki and Lasek (1995c)) are of a similar form. In Fig.9 there is shown a strong edge vortex shedding-up from the main wing. Downwashes in the vicinity of horizontal stabilizer are practically constant and equal to 3°. It means that the gradient $\partial\epsilon/\partial\alpha$ is equal to 0.6.

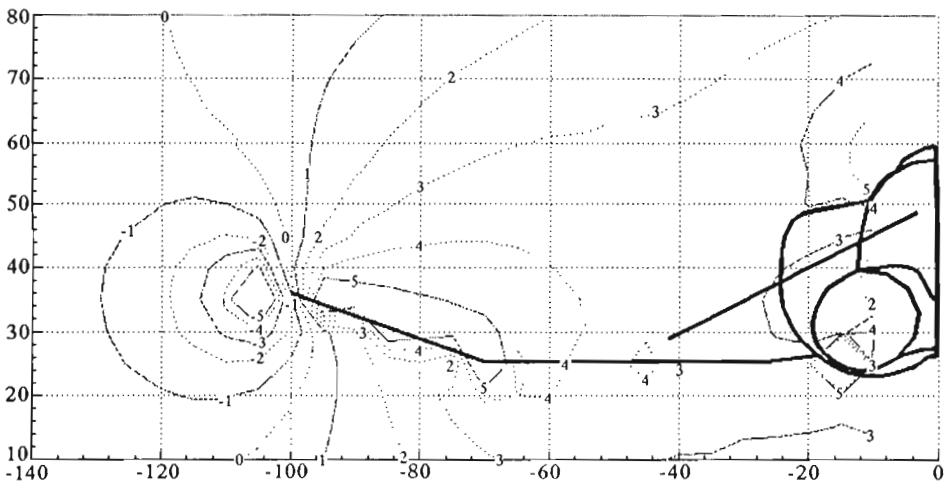

Fig. 9. Downwash izolines for F-4B in the vivinity of the tail

8. Dynamic stability

A stability analysis has been carried out under the assumptions that (1) the aircraft has a plane of symmetry; (2) the angles of sideslip, bank and path are zero and (3) the Mach number and the angle of attack are small. Under such assumptions the differential equations of motion together with kinematic relationships have the form (cf Goraj (1984))

$$\mathbf{M}\frac{d\boldsymbol{x}}{dt} = \mathbf{B}\boldsymbol{x} \tag{8.1}$$

where the mass and generalized stiffness matrices are equal, respectively

$$\mathbf{M} = \begin{bmatrix} m & 0 & 0 & 0 & -mz & 0 & 0 & 0 \\ 0 & m & 0 & mz & 0 & -mz & 0 & 0 \\ 0 & 0 & m - Z_{\dot{w}} & 0 & mx & 0 & 0 & 0 \\ 0 & mz & 0 & J_x & 0 & -J_{xz} & 0 & 0 \\ -mz & 0 & -M_{\dot{w}} & 0 & J_y & 0 & 0 & 0 \\ 0 & -mx & 0 & -J_{xz} & 0 & J_z & 0 & 0 \\ 0 & 0 & 0 & 0 & 0 & 0 & 1 & 0 \\ 0 & 0 & 0 & 0 & 0 & 0 & 0 & 1 \end{bmatrix} \tag{8.2}$$

$$\mathbf{B} = \begin{bmatrix} X_u & 0 & X_w & 0 & X_q & 0 & -G & 0 \\ 0 & Y_v & 0 & Y_p & 0 & Y_r - mV & 0 & G \\ Z_u & 0 & Z_w & 0 & Z_q + mV & 0 & 0 & 0 \\ 0 & L_v & 0 & L_p & 0 & L_r - mzV & 0 & -Gz \\ 0 & 0 & M_w & 0 & M_q + mxV & 0 & Gz & 0 \\ 0 & N_v & 0 & N_p & 0 & N_r + mxV & 0 & -Gx \\ 0 & 0 & 0 & 0 & 1 & 0 & 0 & 0 \\ 0 & 0 & 0 & 1 & 0 & 0 & 0 & 0 \end{bmatrix} \tag{8.3}$$

whilst x, z denote mass center coordinates of an aircraft in the stability frame of reference $Axyz$ (Ax axis is originated in 25% of MAC and directed back of the aircraft along the undisturbed flow velocity), and X_u, X_w, N_p,... – stand for the dimensional stability derivatives computed in the stability frame of reference.

The eigenvalues corresponding to matrix equation (8.1) are

$$\lambda_i = \xi_i + \mathrm{i}\eta_i \tag{8.4}$$

where an imaginary part η_i can be in particular case equal to zero.

In stability analysis one uses various combinations of ξ_i and η_i (cf Nelson (1989)), namely

– damping ratio

$$\zeta = \frac{-\xi}{\sqrt{\xi^2 + \eta^2}} \tag{8.5}$$

– undumped frequency

$$\omega_n = \sqrt{\xi^2 + \eta^2} \tag{8.6}$$

– period of dumped oscillation

$$T = \frac{2\pi}{\eta} \tag{8.7}$$

– time-to-half-amplitude (or time to double amplitude)

$$T_{1/2} = \frac{\ln 2}{-\xi} \tag{8.8}$$

– mode inverse cycles to half amplitude

$$\frac{1}{C_{1/2}} = \frac{T_{1/2}}{T} = \frac{\ln 2}{2\pi}\sqrt{\frac{1-\zeta^2}{\zeta^2}} \tag{8.9}$$

– mode inverse cycles to 1/10 amplitude

$$\frac{1}{C_{1/10}} = \frac{T_{1/10}}{T} = \frac{\ln 10}{2\pi}\sqrt{\frac{1-\zeta^2}{\zeta^2}} \tag{8.10}$$

Most important stability derivatives for the F-4B aircraft, taken from different five sources, are placed in Table 5. The sources are as follows:

1. Numerical package STB (Warsaw University of Technology; available on request from the authors) developed on the basis of simplified engineering data sheets ESDU [25]

2. QL-package (cf Kulicki and Lasek (1995c)) for calculation of pressure distribution by means panel methods

3. NASA Report CR-2144 (cf Heffley and Jewell (1972)) – data for landing configuration

4. NASA Report CR-2144 (cf Heffley and Jewell (1972)) – data for cruising configuration: altitude 10 km, Mach number Ma=0.6

5. NASA Reports TND-6425 (cf Anglin (1971)) and TND-6091 (cf Grafton and Libbey (1971)).

Some derivatives, important from the stability point of view (e.g., the pitching moment derivative m_w) differ depending on the reference it was taken from. It is interesting that even between the results of two NASA Reports TND-6425 and TND-6091, obtained in the same Langley Laboratory in the same year (1970), there exist serious differences in the gradient $dC_L/d\alpha$ (in Fig.5g from TND-6425 we can find this derivative equal to 3.43 1/rad, whereas in Fig.5a from TND-6425 we see that this derivative is equal to 3.27 1/rad). It seems that these differences are caused by the fact that wind-tunnel models corresponded to a bit different project stage of the aircraft and in consequence

they differed in geometry. We can observe dramatically acute difference in the very important derivative l_v, being together with n_v derivative crucial for the lateral stability (l_v in CR-2144 (plot on page 77) at $\alpha = 0$ is equal to -0.088, whereas l_v in TND-6091 (Fig.6 on page 22) at $\alpha = 0$ is equal to -0.046). A relatively high accuracy one can observe comparing the derivative n_v – it changes from the minimum value of 0.13 in TND-6091 (cruising configuration) up to the maximum equal to 0.199 in CR-2144 (landing configuration).

Table 5. Flight conditions: $V = 180\,\mathrm{m/s}$, Ma=0.55, altitude=10 km, $\rho = 0.41\,\mathrm{kg/m^3}$

	STB	QL-PANEL	CR-2144 (cruising conf.)	CR-2144 (landing conf.)	TND-6091 TND-6425
x_u	−0.1040			−0.4840	
x_w	−0.0025			0.5550	
x_q	−0.0037				
z_u	−0.8790				
z_w	−3.0000	−3.5100	−2.8300	−2.8000	−3.2700
z_q	0.2770	7.7400			
$z_{\dot{w}}$	−0.3860				
m_u	−0.0520				
m_w	−0.2970	−0.4510	−0.2200	−0.0980	−0.3460
m_q	−1.5400	−2.6400	−1.2500	−1.0000	−2.0000
$m_{\dot{w}}$	−0.5990			−0.4750	
y_v	−0.3770	−0.6400	−0.6000	−0.6550	−0.6300
y_p	0.1860	−0.1000			
y_r	−0.4710	−0.7750			
l_v	−0.2200	−0.1710	−0.0889	−0.1560	−0.0460
l_p	−0.1380	−0.1920	−0.1110	−0.1360	−0.1000
l_r	0.1190	0.1390	0.0444	0.1030	0.0300
n_v	0.1530	0.1900	0.1170	0.1990	0.1320
n_p	0.0110	0.0225	−0.0039	−0.0065	
n_r	−0.1270	−0.3910	−0.1190	−0.1600	−0.1500

The analysis of dumping and frequency for natural modes of vibration made with the aid of STB package for the aircraft F-4B, using different sets of stability derivatives (given in Table 5) shows that stability characteristics are consistent in quality, and the existing discrepancies have only a quantitative character. In all cases one does not observe the change of stability type, i.e. changing either from stable state into unstable one or vice versa. Scatler of results the parameters ξ and η obtained from different models for short pe-

riod oscillations is rather insignificant. The results obtained from QL-Package model differ most from those from other models, however the difference in the extreme case ($\xi = -0.74$ from QL-Package model and $\xi = -0.44$ from the model with stability derivatives taken from the Report CR-2144) is equal about 40% and seems to be acceptable. Phugoid parameters (especially the dumping coefficient ξ) obtained from various models are very close. Dispersion between the Dutch roll stability coefficients, presented in Fig.10, also can be regarded as acceptable.

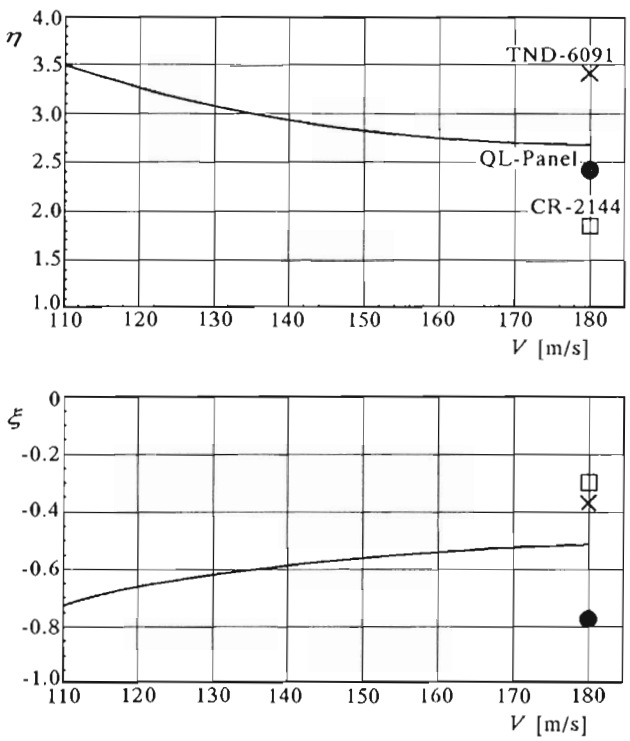

Fig. 10. Damping and frequecy of the Dutch Roll for F-4B

The most important stability characteristics, computed numerically and measured in flight tests, are placed in Table 6. The first seven rows of Table 6 were already analyzed and commented earlier. Most interesting are rows from eighth up to tenth. They present the characteristics $C^{-1}(1/10)$ for short period mode as well as parameters T and $C^{-1}(1/2)$ for the Dutch roll. These characteristics are defined by the aircraft design requirements (for example by FAR) and therefore they should be documented during the certification pro-

cess. The most substantial differences between numerical results obtained from the Report CR-2144 ($C_{SP}^{-1}(1/10) = 0.731$; $T_{DR} = 3.45$; $C_{DR}^{-1}(1/2) = 0.82$, where the index SP denotes short period mode and the index DR corresponds to the Dutch roll mode) and the flight tests results (referred to the flight tests results) are equal to 17% for $C_{SP}^{-1}(1/10)$; 45% for TDR and 57% for $C_{DR}^{-1}(1/2)$, respectively. Differences for short period oscillations are negligible, differences for the Dutch roll are significant and should be eliminated by verification of the stability derivatives.

Table 6

	STB	TND-6091 +STB	CR-2144 flight tests	Derivatives from CR-2144 +STB comput.	QL-Panel +STB
ξ_{SP}	−0.4900	−0.5700		−0.4400	−0.7400
η_{SP}	1.1100	1.2500		0.7300	1.5800
ζ_{SP}	0.4020	0.4100		0.5160	0.4200
ξ_{DR}	−0.5100	−0.3700		−0.3000	−0.7700
η_{DR}	2.6400	3.4100		1.8500	2.4200
ζ_{DR}	0.1880	0.1000		0.1600	0.3000
ξ_{spiral}	−0.1550	−0.1980		−0.0013	−0.0386
$C^{-1}(1/10)_{SP}$	0.8333	0.8600	0.7310	0.6098	0.7813
T_{DR}	2.3600	1.8400	3.4500	3.3900	2.5900
$C^{-1}(1/10)_{DR}$	0.5747	1.0204	0.8200	0.6849	0.3500

9. Conclusion

Panel methods have had significant effect not only on calculating of the pressure distribution over aircraft surfaces but also on the stability investigation. They offer an excellent compromise between reliability, speed and faithful representation of the flow field. First of all, they can be regarded as a very useful tool for determination of the fundamental aerodynamic characteristics of an arbitrary aircraft, especially for the aircraft of strongly coupled aerodynamic configuration. However, one should remember of various limitations: angles of sideslip and angles of attack should be small; flow should be subcritical or pure supersonic; maneuvers can not be too rapid and Reynolds number has to be sufficiently high. Panel methods give opportunity to compute stability derivative, including the rotary stability derivatives. Panel methods also can be used for determination of the neutral points of stability and maneuve-

rability as well as for computing field of downwashes behind the main wing. Accuracy possible to obtain depends on the geometry representation. Usually, it gives acceptable stability characteristics. At last it can be concluded that in many cases the thick fuselage, thin wings and flat wake model gives very high accuracy, especially if we consider the stability characteristics.

References

1. ANGLIN E.L., 1971, Static Force Tests of a Model of a Twin-Jet Fighter Airplane for Angles of Attack from $-10°$ to $110°$ and Sideslip Angles from $-40°$ to $40°$, *NASA TND-6425,* Washington D.C., Aug.
2. BERTIN J., SMITH M., 1989, *Aerodynamics for Engineers,* Prentice-Hall Inc., Singapore
3. BŁASZCZYK P., 1996, Numerical Aspects of Modelling of Surface Geometry on Panel Methods Needs (in polish), *Transactions of Silesian University of Technology - Chair of Technical Mechanics,* **1**, Gliwice, 31-36
4. GOETZENDORF-GRABOWSKI T., GORAJ Z., 1996, Calculating of Stability Characteristics of an Aircraft in Subsonic Flow Using Panel Methods (in polish), *Transactions of the Institute of Aviation - Scientific Quarterly,* 145, Warszawa, 31-49
5. GORAJ Z., 1984, *Calculations of Equilibrium, Maneuverability and Stability of an Aircraft in Subsonic Range of Speed* (in polish), Warsaw University of Technology, Warszawa
6. GORAJ Z., 1993, Determination of Neutral Points of an Aircraft Stability by Use VLM (in polish), *Transactions of Silesian University of Technology, (Mechanics),* **113**, Gliwice, 101-109
7. GORAJ Z., PIETRUCHA J., 1993, Modifications of Potential Flow Model for Panel Method Improvement (in polish), *Transactions of the Institute of Aviation - Scientific Quarterly,* 135, Warszawa, 27-44
8. GORAJ Z., PIETRUCHA J., 1994a, Calculation of the Stability Derivatives about Steady Flight Path after Sudden Acceleration Using Vortex Rings (in polish), *Proceedings of the XI All-Polish Conference on Fluid Mechanics,* part I, Warszawa 17-21 Oct., 37-42
9. GORAJ Z., PIETRUCHA J., 1994b, Mathematical Modelling of Selected Maneuvres of an Aircraft Using Modified Vortex Lattice Method, *19th Congress of the International Council of the Aeronautical Sciences,* 18-24 Sept., Anaheim-California, 1211-1221
10. GORAJ Z., PIETRUCHA J., 1995a, Classical Panel Methods - a Routine Tool for Aerodynamic Calculations of Complex Aircraft Configurations: from Con-Cepts to Codes, *J. Theor. Appl. Mech.,* **33**, 4, 843-878
11. GORAJ Z., PIETRUCHA P., 1995b, Physical Modelling of Important Flow Phenomena in Aircraft Aerodynamics, *Proceedings of Institute of Aviation,* **140**, 1, 13-47

12. GORAJ Z., SZNAJDER J., 1995, Panel Methods in Flight Mechanics – Possibilities and Limitations (in polish), *Transactions of the Institute of Aviation – Scientific Quarterly,* 143, Warszawa, 59-102

13. GORAJ Z., BŁASZCZYK P., GOETZENDORF-GRABOWSKI T., KULICKI P., LASEK M., WINNICKI J., 1996, Stability Investigation into Complex Aerodynamic Configurations, Raport of Institute of Aviation (for State Committee for Scientific Research – grant No. (S 604 028 04, in polish), Warszawa

14. GRAFTON S.B., LIBBEY CH.E., 1971, Dynamic Stability Derivatives of a Twin-Jet Fighter Model for Angles of Attack from -10 to 110 deg, *NASA TN D-6091,* Washington D.C., Jan.

15. HEFFLEY R.K., JEWELL W.F., 1972, Aircraft Handling Qualities Data, *NASA CR-2144,* Washington D.C., Dec.

16. HESS J.L., 1972, Calculation of Potential Flow about Three-Dimensional Lifting Bodies, *Final Technical Report,* McDonnell Douglas Report No. MOC J5679-01, Oct.

17. HESS J.L., SMITH A.M.O., 1966, Calculation of Potential Flow about Arbitrary Bodies, *Progress in Aeronautical Sciences,* **8**

18. KATZ J., PLOTTKIN A., 1991, *Low-Specd Aerodynamics – from Wing Theory to Panel Methods,* McGraw-Hill, Inc.

19. KUBRYŃSKI K., 1995, Application of the Subsonic Panel Method to Aerodynamic Analysis and Design, *Proc. First Seminar on Resent Research and Design Progress in Aeronautical Engineering and its Influence on Education,* Edit. Z.Goraj, *Bul.4 of IAAM Warsaw Univ.Tech.,* Warszawa, 131-137

20. KULICKI P., LASEK M., 1995a, Determination of a Lift Curve Slope for Wing-body Configuration by Means of Low order Panel Methods (in polish), *Proceedings of Polish Society of Theoretical and Applied Mechanics,* Warszawa, 311-319

21. KULICKI P., LASEK M., 1995b, Implementation of the Panel Method for the Wing-Body Aerodynamic Center Determination, (in polish), *Transactions of Silesian University of Technology, (Mechanics),* **122**, Gliwice, 153-157

22. KULICKI P., LASEK M., 1995c, QL-Panel – Package for Computing of Pressure Distribution over Lifting Surfaces Using hess Method of Low Order (in polish), *Report in Institute of Aviation,* Warsaw

23. KONSTANDINOPOULOS P. ET AL., 1995, A Vortex Lattice Method for General, Unsteady Aerodynamics, *Jour. of Aircraft,* **22**, 1, 43-49

24. NELSON R., 1989, *Flight Stability and Automatic Control,* McGraw-Hill Book Company

25. ROSKAM J., 1985, *Airplane Design,* Roskam Aviation and Engineering Corp., Ottawa, KS

26. ESDU (Engineering Sciences Data Unit). Aerodynamics Sub-Serie. Royal Aeronautical Society, 251-259 Regent Street, London W1R 7AD, England

Analiza stateczności samolotu o konfiguracji aerodynamicznej silnie sprzężonej

Streszczenie

W pracy przedstawiono zastosowanie metod panelowych do analizy stateczności dynamicznej samolotu. Dokonano przeglądu najważniejszych metod i przedyskutowano ich podstawy matematyczne (równania rządzące, postaci warunków brzegowych, metody dyskretyzacji) mające największy wpływ na efektywność kodów obliczeniowych, umożliwiających wyznaczenie rozkładów ciśnienia nad powierzchniami nienośnymi (kadłubami, gondolami) oraz nośnymi (płatami, usterzeniami). Przedstawiono wybrane procedury obliczeń charakterystyk statycznych i dynamicznych, decydujących o stateczności samolotu. W szczególności omówiono wyznaczanie kątów odchylenia strug za płatem, punkty neutralne stateczności i sterowności statycznej oraz pochodne aerodynamiczne stateczności. W pracy zamieszczono wyniki obliczeń przykładowych, uzyskanych metodami panelowymi i porównano je z wynikami pomiarów w tunelach aerodynamicznych oraz z wynikami testów w locie.

Manuscript received June 21, 1996; accepted for print September 11, 1996